JOURNAL OF SOLID STATE CHEMISTRY 73, 57–64 (1988)

A Mössbauer Spectroscopy Study of the $CaFe_xMn_{1-x}O_{3-y}$ Ferrites ($0.2 \leq X \leq 0.4$)

J. RODRIGUEZ

Instituto de Ciencia de Materiales de Barcelona, CSIC, Martí i Franqués s/n, Barcelona 08028, Spain

J. FONTCUBERTA

Departamento de Física Fundamental, División de Ciencis de la Universidad de Barcelona, Diagonal 645, Barcelona 08028, Spain

G. LONGWORTH

Nuclear Physics, AERE Harwell, Oxfordshire OX11 ORA, United Kingdom

AND M. VALLET-REGÍ AND J. M. GONZÁLEZ-CALBET*

Departamento de Química Inorgánica, Facultad de Químicas, Universidad Complutense, Madrid 28040, Spain

Received October 27, 1986; in revised form May 29, 1987

$CaFe_xMn_{1-x}O_{3-y}$ samples prepared in air contain several types of intergrowing microdomains as observed by electron microscopy. Using Mössbauer spectroscopy we have proved the existence of three differently coordinated Fe(+3) cations. A model for microdomain composition and distribution that accounts well for the present Mössbauer results and for previous electron microscopy data is proposed.

Introduction

Compositional variations in crystalline materials may lead in some cases to very complex structural arrangements due to the various possibilities for distributing anionic vacancies. Thus, several electron diffraction (ED) and electron microscopy (EM) studies of some perovskite related oxides, of general formula $AFeO_{3-y}$ (A = Ca, Sr, La, Nd . . .), have shown that the accommodation of nonstoichiometry occurs through the formation of three-dimensional (3D) microdomains (*1–3*).

In the $CaFe_xMn_{1-x}O_{3-y}$ system the coexistence of Fe and Mn cations with different oxidation states should produce an even more complicated situation. Vallet-Regí *et al.* (*4*) recently reported ED and EM studies of the x = 0.2, 0.3, 0.4 members of this series.

To illustrate the complexity of these oxides and to help in a better understanding of our own results we summarize some of the

* To whom all correspondence should be addressed.

0022-4596/88 $3.00

results obtained for the $x = 0.2$ and 0.4 members.

For the $x = 0.2$ sample the X-ray powder diffraction (XRPD), ED, and EM results of Vallet-Regí *et al.* (*4*) were interpreted on the basis of a random vacancy distribution in the sample. The patterns could be indexed in a tetragonal unit cell ($a_c\sqrt{2} \times a_c\sqrt{2} \times 2a_c$), where a_c is the cell parameter of the cubic perovskite substructure. The doubled c axis ($2a_c \simeq 7.5$ Å) was attributed to the tilting of octahedra along the c axis, as found in $CaMnO_3$ (*5*). In addition, ED shows that the doubling-cell direction was not uniform over the crystals but that three coexisting different orientations were observed, giving rise to a 3D microdomain texture. In what follows the $CaMnO_3$-type domains will be denoted by perovskite-type domains (PTD).

For the $x = 0.4$ sample, PTD analogous to those found for $x = 0.2$ were encountered. However, ED and EM also revealed the presence of small brownmillerite-type ($a_c\sqrt{2} \times 4a_c \times a_c\sqrt{2}$) domains (BTD), with their b axis alternating at random along the ⟨100⟩ directions. Inside the BTD the metallic cations are octahedrally and tetrahedrally coordinated in the 1 : 1 ratio (*6*). The BTD may be considered to form linked octahedron–tetrahedron (OT) units.

The XRPD technique is unable to detect such small BTD and only shows the reflections corresponding to the perovskite substructure: The average linear dimension of the microdomains (~70 Å) and the relatively low scattering factor of oxygen produce broad and very weak reflections.

From this analysis it follows that oxygen vacancies are randomly distributed in PTD but organized in regular arrays in BTD, thus leading to some differences in local composition through the crystals.

For a deeper comprehension of the relationships between composition and the microdomain structure, a technique yielding microscopic information is desirable. Mössbauer spectroscopy (MS) is a local probe, particularly suited for analyzing these materials. In this paper we report a MS study of the $CaFe_xMn_{1-x}O_{3-y}$ system in the $0.2 \leq x \leq 0.4$ range.

From the analysis of the spectra we can document the existence of three differently coordinated Fe(+3) cations. In addition, by using previously reported data from chemical analysis and our own present MS results, we have determined the relative concentration of the two types of microdomains present in the samples. Our results are in good agreement with the existing ED and EM data.

Finally, the vacancy distribution in PTD is revised. We show that the previously observed tetragonal cell is also compatible with a particular vacancy ordering; our proposed model accounts well for all existing data on this system. The present paper represents, as far as we know, the first attempt to interpret MS data on the basis of a microdomain textured material.

Experimental

Full details for $CaFe_xMn_{1-x}O_{3-y}$ ($0.2 \leq x \leq 0.4$) sample preparation, chemical analysis, XRPD, ED, and EM are given in Ref. (*4*). X-ray and chemical analysis data are summarized in Table I.

MS of powdered samples were performed on a conventional spectrometer with constant acceleration and Co-57 : Rh source. Isomer shifts (IS) are referred to α-Fe. The spectra have been fitted by using the MOSFUN program (*7*). No constraints have been included in the fitting procedure except for the intensity ratio of the lines in a given magnetic (3 : 2 : 1 : 2 : 3) or quadrupolar (1 : 1) subspectrum.

Results

Room temperature Mössbauer spectra of $CaFe_xMn_{1-x}O_{3-y}$ ($x = 0.2, 0.3, 0.4$) samples

TABLE I

CHEMICAL ANALYSIS DATA AND UNIT CELL PARAMETERS OF THE DIFFERENT SAMPLES

x (nom)	Chemical composition	a(Å)	b(Å)	c(Å)	a_c[a]
0.2	$CaFe^{+3}_{0.20}Mn^{+3}_{0.35}Mn^{+4}_{0.45}O_{2.72}$	5.307(1)	7.405(1)	5.307(1)	3.753
0.3	$CaFe^{+3}_{0.30}Mn^{+3}_{0.24}Mn^{+4}_{0.46}O_{2.73}$	5.313(1)	7.514(1)	5.313(1)	3.757
0.4	$CaFe^{+3}_{0.40}Mn^{+3}_{0.22}Mn^{+4}_{0.38}O_{2.69}$	3.776(1)	—	—	3.776

[a] a_c refers to the pseudocubic unit cell parameter.

do not show any magnetic order. Only complex quadrupole-split spectra are observed (Fig. 1). At 4.2 K, magnetic order is established through the samples and the spectra exhibit a complex mixture of unresolved magnetic hyperfine sextets (Fig. 2). As we are mainly interested in structural properties, the room temperature spectra will be easier to analyze and should provide better information. Therefore, we focus on room temperature data.

Paramagnetic Mössbauer spectra were fitted with three quadrupole subspectra as shown in Fig. 1. The corresponding hyperfine parameters are given in Table II. The IS of all the components are characteristic of only one oxidation state for the iron cations (+3) located at three different sites: subspectra 1, 2, and 3 correspond to Fe(+3) in VI (octahedral), V (fivefold), and IV (tetrahedral) coordination (*8*), respectively. The quadrupole splittings (QS) are in the sequence: $QS_{VI} < QS_V < QS_{IV}$.

The IS and QS (in mm/sec) observed in $Ca_3Fe_{1.65}Mn_{1.35}O_{8.02}$ synthesized by Nguyen *et al.* (*9*) are $(IS, QS)_{OCT} = (0.33, 0.69)$ and $(IS, QS)_{TET} = (0.18, 1.41)$, where OCT and TET stand for octahedral and tetrahedral environments, respectively. In our case, the average values of the 1 and 3 components are $(IS, QS)_{OCT} = (0.32, 0.52)$ and $(IS, QS)_{TET} = (0.18, 1.46)$. However, for component 2 these values are $(IS, QS)_V = (0.28, 1.07)$. The existence of high anionic vacancy concentration in our samples, and the intermediate IS value of the second

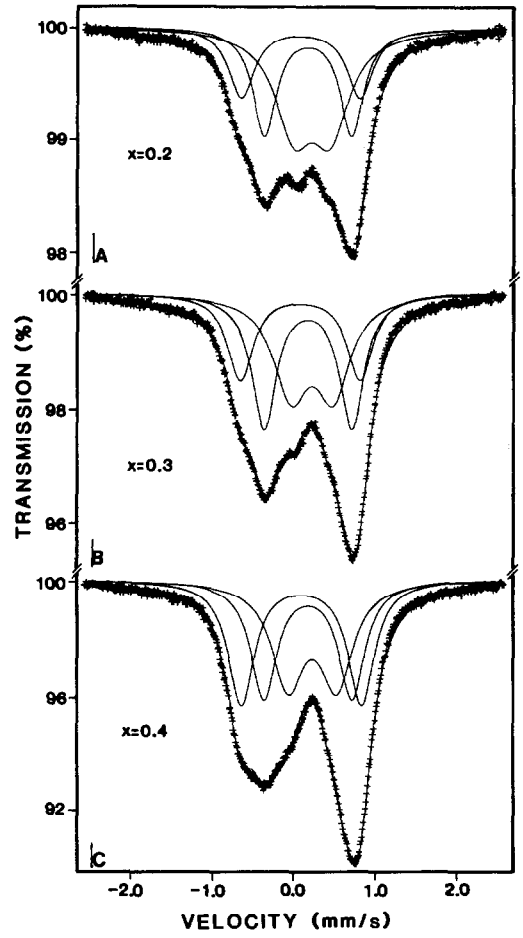

FIG. 1. Mössbauer spectra performed at room temperature of the (A) $x = 0.20$, (B) $x = 0.30$, and (C) $x = 0.40$ samples.

TABLE II

MÖSSBAUER PARAMETERS OF THE SPECTRA RECORDED AT ROOM TEMPERATURE

x	I_1[a]	I_2	I_3	IS_1	IS_2	IS_3
0.2	45(4)	32(4)	23(3)	0.319(4)	0.278(5)	0.181(8)
0.3	37(4)	37(5)	26(3)	0.322(5)	0.277(4)	0.181(7)
0.4	34(4)	32(6)	34(3)	0.326(5)	0.279(5)	0.192(5)
	QS_1	QS_2	QS_3	A_1	A_2	A_3
0.2	0.45(2)	1.06(1)	1.44(2)	0.56(4)	0.34(3)	0.38(3)
0.3	0.52(2)	1.07(1)	1.46(1)	0.51(3)	0.36(3)	0.38(2)
0.4	0.60(2)	1.08(2)	1.47(1)	0.47(2)	0.38(4)	0.38(2)

[a] I, IS, QS, and A stand for the line intensity, isomer shift, quadrupole splitting, and linewidth, respectively. Line intensities are given in percentage; the rest of the parameters are in millimeters per second.

component of the spectra, allow us to attribute the 0.28 mm/sec line to Fe(+3) in V coordination, although we cannot distinguish between square pyramids or trigonal bipyramids.

Spectra recorded at 4.2 K can also be fitted by using three magnetic sextets and assuming a distribution of magnetic hyperfine fields for each. The existence of different paramagnetic cations and its chemical disorder can be invoked to account for the magnetic field distribution which was assumed to be Lorentzian. Figure 2 shows the fitted spectra, and Table III summarizes the obtained relevant parameters.

As a result of the strong line overlap it is difficult to obtain reliable intensity values from these low-temperature spectra, even though low-temperature and room temperature fitted intensity values are the same within experimental error, except for the subspectrum 1 of the $x = 0.2$ sample. The overlap is also responsible for the absence of scaling of the hyperfine fields with x. The fitted quadrupole constant (ε) values are essentially zero. In fact, this result should have been expected in our highly disordered system. The local variations of the angle between the principal direction of the electric field gradient and the hyperfine

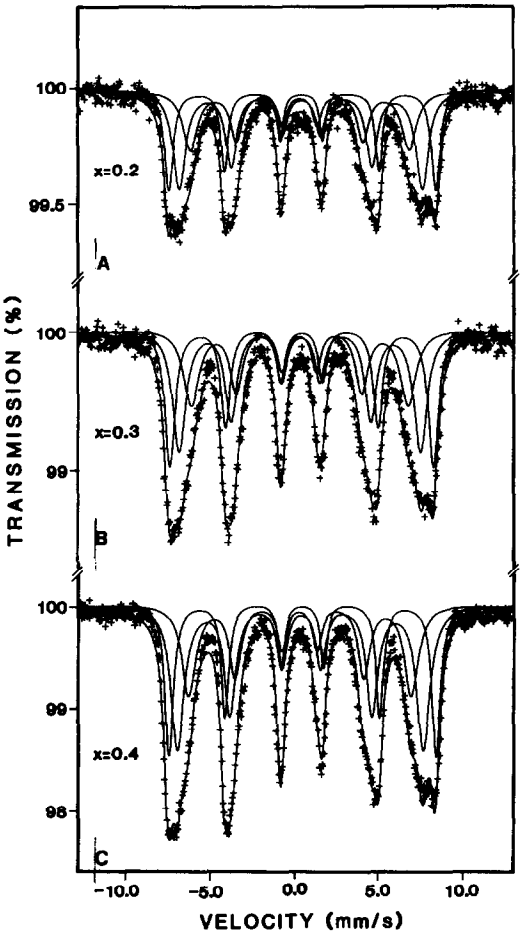

FIG. 2. Mössbauer spectra performed at 4.2 K of the (A) $x = 0.20$, (B) $x = 0.30$, and (C) $x = 0.40$ samples.

TABLE III

MÖSSBAUER PARAMETERS OF THE SPECTRA RECORDED AT 4.2 K

x	I_1	I_2	I_3	IS_1	IS_2	IS_3
0.2	30(6)	41(15)	29(11)	0.46(1)	0.43(2)	0.33(3)
0.3	33(8)	39(18)	28(11)	0.45(1)	0.41(2)	0.31(3)
0.4	29(6)	43(4)	29(9)	0.47(2)	0.41(2)	0.30(3)
	H_1[a]	H_2	H_3			
0.2	492(2)	448(3)	403(5)			
0.3	485(2)	445(3)	399(6)			
0.4	492(1)	453(3)	410(4)			

[a] The hyperfine magnetic fields (H_1) are given in KOe.

magnetic field average the measured quadrupole constants to zero.

Discussion

The line intensity data from spectra recorded at room temperature, as mentioned above, are more reliable than the corresponding analyses based on low-temperature spectra. Figure 1 and Table II show an increase in the Fe_{TET} amount with x composition. As pointed out in the Introduction, tetrahedrally coordinated metallic cations are only present in the OT units. Therefore, our results suggest that the relative number of OT units in the samples should increase as the Fe content (x) is raised. This fact is in agreement with the results obtained by ED and EM, where BTD could be observed only for the $x = 0.4$ sample (*4*).

As shown below, these domains must also be present in the $x = 0.2$ and $x = 0.3$ samples, but since they are at lower concentrations they cannot be detected by ED, because BTD is built up from OT units (an octahedron sharing a corner with a tetrahedron). From electrostatic stability arguments, it is reasonable to assume that every tetrahedron is always connected to at least one octahedron. Associated with this OT unit there is always a region of local composition $A_2M_2O_5$. By linking OT units one can build 1D, 2D, and 3D networks with $A_2M_2O_5$ composition, and, eventually, construct BTDs. If the number of OT units is high enough, they can be spatially arranged in long-range order to produce the corresponding diffraction peaks. Also, isolated short-range ordered OT units, distributed over the whole crystal, can produce diffraction maxima if their arrangement has the degree of coherence and periodicity matching the incident radiation.

In fact, inspection of EM photographs for the $x = 0.4$ sample (Fig. 3) reveals the existence of isolated OT, linked in planes, as well as 3D short-range ordered OT units, leading to BTD. When the coherence conditions between a set of BTD are fulfilled the corresponding maxima are observed in the ED pattern. Of course, the observation of the superstructure peaks is not possible if the concentration of OT units in the sample is small, as seems to occur for $x = 0.2$ and $x = 0.3$ when using either ED or XRPD. The existence of isolated OT units or small BTD is also supported by the absence of the hyperfine magnetic splitting characteristic of room temperature $Ca_2Fe_2O_5$ (*10*).

So far we have only discussed vacancy ordering in terms of stacking octahedron and tetrahedron polyhedra. However, as our Mössbauer results show, oxygen vacancies in a perovskite net lead to fivefold coordination coexisting with octahedrally coordinated cations. Therefore, we can assume that the samples are essentially formed by a combination of OT units (which eventually give to BTD) and the PTD which contain octahedrally coordinated and fivefold coordinated cations. We can write down a structural formula which reflects this situation:

$$CaMn^{+3}_{1-x-z}Mn^{+4}_{z}Fe^{OCT}_{x-t-v}Fe^{V}_{v}Fe^{TET}_{t}O_{3-y} \rightarrow q(CaMn^{+3}_{0.5-m}Fe^{OCT}_{m}Fe^{TET}_{0.5}O_{2.5})_{OT} + (1-q)(CaMn^{+3}_{1-p-r}Mn^{+4}_{r}Fe^{OCT}_{p-w}Fe^{V}_{w}O_{3-\delta})_{PTD}, \quad (1)$$

where q stands for the fraction of OT units present in the sample.

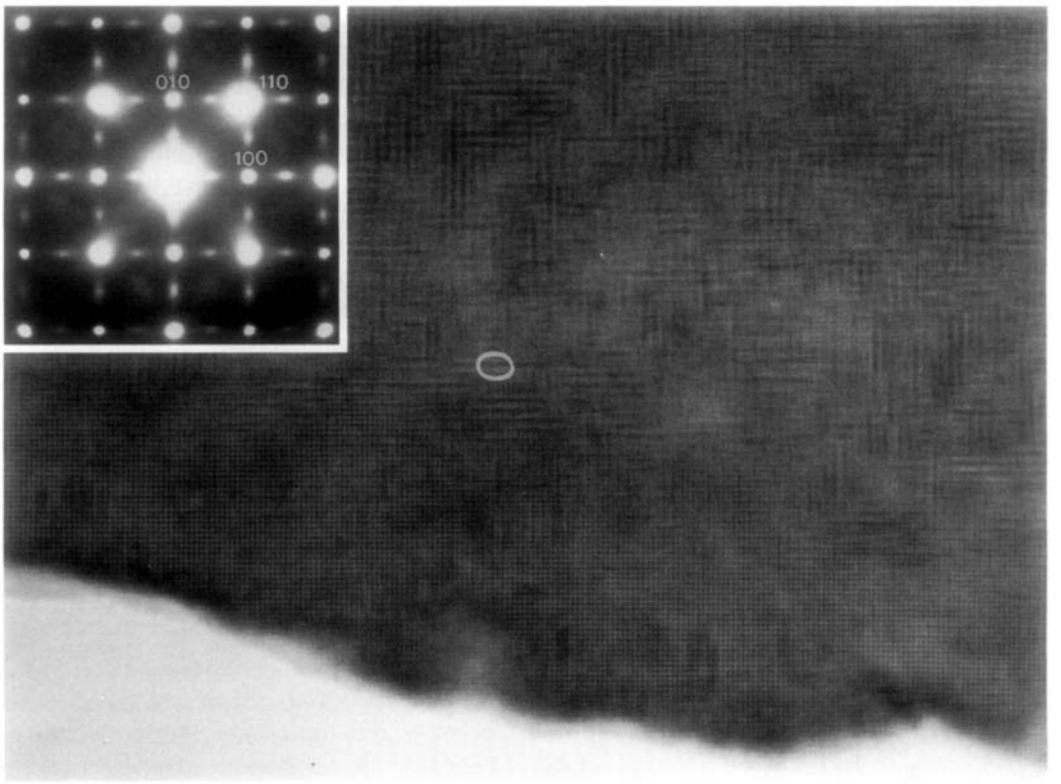

FIG. 3. Electron micrograph and corresponding electron diffraction pattern of the $CaFe^{+3}_{0.40}Mn^{+3}_{0.22}Mn^{+4}_{0.38}O_{2.69}$ sample along the $[001]_c$ zone axis. Brownmillerite-type domains, showing d spacings of 7.4 Å, are intergrown with perovskite-type domains. The encircled zone shows an isolated OT layer.

The overall anionic vacancy concentration (y), the total iron contents (x), and the Mn(+4) concentration (z) are known from chemical analysis (Table I). The concentrations $x - t - v$, v, and t, refer to Fe(+3) cations in octahedral, fivefold, and tetrahedral coordinations, respectively, and can be deduced from the Mössbauer spectra ($v = x \cdot I_2/100$, $t = x \cdot I_3/100$, see Table II).

From electroneutrality in PTD and from the equivalence of the two members of the Eq. (1), the following system of five independent equations with six unknown parameters can be established:

$$r = 1 - 2\delta \tag{2}$$

$$v = (1 - q)w \tag{3}$$

$$z = (1 - q)r \tag{4}$$

$$t = \tfrac{1}{2} q \tag{5}$$

$$x = q(m + \tfrac{1}{2}) + (1 - q)p, \tag{6}$$

where m and p remain undetermined but connected by Eq. (6). Using the chemical analysis data from Table I, our Mössbauer data (Table II), and Eqs. (2)–(6), we can deduce the relative concentration of OT units (q) and PTD ($1 - q$) in the sample; the oxygen contents ($3 - \delta$), and the relative concentrations of Mn(+4) (r) and fivefold coordinated Fe(w) in the PTD. Table IV summarizes the calculated results.

From inspection of the results in Table IV, two points are of special interest:

(1) The relative amount of the OT units existing in the samples increases from $q \simeq 10\%$ for $x = 0.2$ to $q \simeq 30\%$ for $x = 0.4$.

TABLE IV

PARAMETERS OBTAINED FROM THE SOLUTION OF Eqs. (2), (3), (4), AND (5)

x	q	r	w	δ
0.20	0.09(1)	0.50(1)	0.07(1)	0.252(7)
0.30	0.15(2)	0.55(2)	0.13(2)	0.228(9)
0.40	0.27(2)	0.52(2)	0.18(3)	0.24(1)

Note. Errors in parentheses are calculated assuming $\sigma(x) = \sigma(z) = 0.01$ and using the intensity errors given in Table II.

Since BTD were not observed for $x = 0.2$ and $x = 0.3$ by ED (*4*), we conclude that in these samples OT units are isolated entities oriented at random along the $\langle 100 \rangle_c$ directions of the perovskite substructure. Therefore, observation of the characteristic reflections of the brownmillerite structure is only possible if a large number of OT units occur in BTD. For $x = 0.4$, BTD are clearly seen in ED and EM images (see Fig. 3).

(2) On the other hand this analysis yields the number of anionic vacancies of the PTD. In all cases the number of vacancies is close to $\delta = 0.25$, indicating that the composition of PTD is close to $AMO_{2.75}$.

In the previous work (*4*), it was found that superlattice reflections appearing in ED patterns of the $x = 0.2$ sample were indexed in a tetragonal ($a_c\sqrt{2} \times a_c\sqrt{2} \times 2a_c$) unit cell, the doubled perovskite axis being randomly oriented along the three space directions. Twinning was assumed to be caused by the slight distortion produced by the tilt of octahedra, as has already been shown to occur in $LaFeO_3$ (*11, 12*) and $SrSnO_3$ (*13*).

However, the total number of vacancies ($\delta \simeq 0.25$) in PTD (containing only octahedral and fivefold coordinated cations) suggests that oxygen vacancies can be regularly distributed through the perovskite lattice. In fact, it is possible to construct a model of vacancy ordering that leads to a doubled cell, as observed. This model would be built up from alternated octahedral and pyramidal (either square or trigonal bypiramids) layers, as shown in Fig. 4. The model has the unit cell and composition experimentally observed. In order to preserve the twinned structure the doubled axis alternates at random in $\langle 100 \rangle$ directions. However, Reller *et al.* (*14*) have observed a different vacancy ordering in $CaMnO_{2.75}$ which does not correspond with our experimental data.

Assuming this model of vacancy ordering (Fig. 4), we can estimate the values of m and p in Eq. (6). It is well known that Mn(+4) cations have a stronger preference for octahedral coordination than Fe(+3) or Mn(+3) cations; therefore, we assume that Mn(+4) occupies the octahedral layers shown in Fig. 4. It follows that the Fe^{OCT} concentration in PTD must be minimal. Taking into account that Mn(+4) concentration (r) is always close to 0.5 (see Table IV), the minimal Fe^{OCT} concentration, in PTD, is reached for maximum m value ($m = 0.5$, Fe^{OCT} in OT units). In that case the OT units have the $Ca_2Fe_2O_5$ composition and $p = (x - q)/(1 - q)$. Using the x and q values from Table IV the composition de-

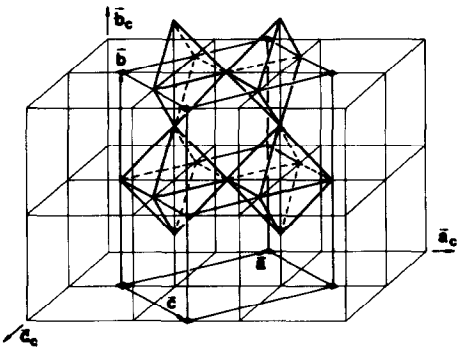

FIG. 4. Idealized structure of a perovskite-type domain of $AMO_{2.75}$ composition, in which octahedra layers alternate with square pyramidal layers. The relationship between the unit cell and the cubic perovskite substructure is $a_c\sqrt{2} \times a_c\sqrt{2} \times 2a_c$.

duced for each sample is

$x = 0.2$: $0.09(CaFeO_{2.5})_{OT} + 0.91(CaMn^{+3}_{0.38}Mn^{+4}_{0.50}Fe^{OCT}_{0.05}Fe^{V}_{0.07}O_{2.75})_{PTD}$

$x = 0.3$: $0.15(CaFeO_{2.5})_{OT} + 0.85(CaMn^{+3}_{0.28}Mn^{+4}_{0.55}Fe^{OCT}_{0.04}Fe^{V}_{0.13}O_{2.77})_{PTD}$

$x = 0.4$: $0.27(CaFeO_{2.5})_{OT} + 0.73(CaMn^{+3}_{0.30}Mn^{+4}_{0.52}Fe^{V}_{0.18}O_{2.76})_{PTD}$.

In the $x = 0.2$ sample the errors associated with the calculated compositional parameters lead to a ratio $OCT/V \simeq 1.2$ slightly greater than the exact value ($OCT/V = 1$) for $\delta = 0.25$.

In the $x = 0.4$ sample, all the Fe^{TET} observed by MS arise, exclusively, from the $Ca_2Fe_2O_5$-like domains. However, the hyperfine magnetic spectrum characteristic of $Ca_2Fe_2O_5$ (*10*) is not observed. As we have already noted, the BTD are small entities formed by OT units and the magnetic spectrum disappears due to superparamagnetic relaxation.

From our analysis it follows that for $x > 0.4$, where the concentration of BTD should be larger, the cooperative magnetic ordering between the OT units should be established at room temperature by avoiding any superparamagnetic effect. In fact, preliminary measurements on the $x = 0.5$ sample have revealed the appearance of magnetic splitting at room temperature, coexisting with paramagnetic quadrupole-split subspectra, which is of the same type as that in $Ca_2Fe_2O_5$. Further work is being carried out in order to clarify this final point.

Acknowledgment

We thank the CAICYT (Spain) for financial support.

References

1. M. A. ALARIO, J. C. JOUBERT, AND J. P. LEVY, *Mater. Res. Bull.* **17,** 733 (1982).
2. M. A. ALARIO, M. J. R. HENCHE, M. VALLET, J. M. G. CALBET, J. C. GRENIER, A. WATTIAUX, AND P. HAGENMULLER, *J. Solid State Chem.* **46,** 23 (1983).
3. M. A. ALARIO, J. M. GONZÁLEZ-CALBET, M. VALLET-REGÍ, AND J. C. GRENIER, *J. Solid State Chem.* **49,** 219 (1983).
4. M. VALLET-REGÍ, J. M. GONZÁLEZ-CALBET, J. VERDE, AND M. A. ALARIO, *J. Solid State Chem.* **57,** 197 (1985).
5. K. R. POEPPELMEIER, M. E. LEONOWICZ, J. C. SCANLON, J. M. LONGO, AND W. B. YELON, *J. Solid State Chem.* **45,** 71 (1982).
6. A. A. COLVILLE, *Acta Crystallogr.* **B26,** 1469 (1970).
7. E. W. MÜLLER, "MOSFUN: A New and Versatile Mössbauer Fitting Program," Institut für Anorganische Chemie und Analytische Chemie. Johannes Gutenberg-Universitat. Distributed by Mössbauer Effect Data Center, University of North Carolina, Asheville (1980).
8. F. MENIL, *J. Phys. Chem. Solids* **46**(7), 763 (1985).
9. N. NGUYEN, Y. CALAGE, F. VARRET, G. FEREY, V. CAIGNAERT, M. HERVIEU, AND B. RAVEAU, *J. Solid State Chem.* **53,** 398 (1984).
10. S. GELLER, R. W. GRANT, AND U. GONSER, *Prog. Solid State Chem.* **5,** 5 (1971).
11. M. VALLET-REGÍ, J. GONZÁLEZ-CALBET, M. A. ALARIO, J. C. GRENIER, AND P. HAGENMULLER, *J. Solid State Chem.* **55,** 251 (1984).
12. M. MAREZIO AND P. D. DERNIER, *Mater. Res. Bull.* **6,** 23 (1971).
13. A. VEGAS, M. VALLET-REGÍ, J. M. GONZÁLEZ-CALBET, AND M. A. ALARIO, *Acta Crystallogr. B* **42,** 167 (1986).
14. A. RELLER, J. M. THOMAS, D. A. JEFFERSON, AND M. K. UPPAL, *Proc. R. Soc. London, Ser. A* **394,** 223 (1984).